

Interactive comment on “Understanding the Mechanism of Arctic Amplification and Sea Ice Loss” by Kwang-Yul Kim et al.

Kwang-Yul Kim et al.

kwang56@snu.ac.kr

Received and published: 7 July 2017

Response to the Comments of Reviewer 1

The manuscript attempts to address the mechanisms of Arctic amplification of climate warming and sea ice loss. Cyclostationary empirical orthogonal functions are applied on ERA-Interim reanalysis products, and the methodology includes novel aspects. Some interesting results are found on the relationships between turbulent surface fluxes, longwave radiation, and sea ice loss. After substantial revisions the manuscript has potential for a good paper in The Cryosphere.

Major comments

Comment1(C1): The authors focus on the statistical relationships of the spatial pat-
C1

terns of anomalies in wintertime sea ice concentration, turbulent surface fluxes of sensible and latent heat, upward and downward longwave radiation, as well as air temperature, humidity and total cloud cover. Both the Arctic amplification and sea ice loss are, however, much more complicated processes, involving many factors, such as the large-scale atmospheric transports of heat and moisture from lower latitudes to the Arctic, and oceanic transports of heat and freshwater. Also, the role of clouds in the Arctic climate system cannot be characterized simply by the total cloud cover; the cloud water and ice contents are at least equally important, as are also the complex interactions between the surface fluxes, boundary-layer turbulence, cloud physics and radiative transfer. I don't mean that the authors should address all these processes, but they should make it clear in the manuscript that they restrict to processes acting in the Arctic, ignoring the forcing from lower latitudes, and they should pay more attention to cloud water and ice contents, which are physically more meaningful variables than the total cloud cover based on reanalysis.

Response1(R1): We thank the reviewer for detailed and constructive comments on the manuscript. As the reviewer mentioned, there are other processes, particularly forcing from lower latitudes, which are important for Arctic amplification and sea ice reduction. As can be seen in Figure R1, there is a net convergence of moisture transport and heat transport over the region of sea ice reduction, although the center of action is over the Greenland Sea. Thus, moisture and heat transport from lower latitudes apparently affects the variation of sea ice concentration. Figure R2 further shows that there is an appreciable correlation between the specific humidity variation and convergence of moisture transport ($\text{corr}=0.62$) and between the lower tropospheric temperature and convergence of heat transport ($\text{corr}=0.33$). Thus, it seems that both the convergence of moisture transport and the convergence of heat transport are at least partly responsible for the variation of specific humidity and temperature in the lower troposphere. On the other hand, the convergence of horizontal transport of moisture cannot explain one essential element of specific humidity anomaly - the mean of anomalous specific humidity. As can be seen in Figure R2a, the mean of moisture convergence is close to
C2

0.6×10^{-6} g/kg/sec, which amounts to ~ 0.05 g/kg of moisture. This value explains only about 17% of the mean value of anomalous specific humidity (~ 0.3 g/kg); the remainder should derive from a vertical process. Consider the following moisture conservation equation:

$$\frac{\partial q}{\partial t} = -\vec{u} \cdot \nabla q + S \doteq -\nabla \cdot (q\vec{u}) + S = -\nabla_h \cdot (q\vec{u}) - \frac{\partial(qw)}{\partial z} + S.$$

The convergence of the horizontal moisture transport is not so effective as the convergence of the vertical moisture transport in the equation above. As can be seen in Fig. R3, the anomalous evaporation due to sea ice reduction is positive throughout the winter and its magnitude is reasonable in comparison with the increase in specific humidity. The two time series in Fig. R3 are negatively correlated (except for the mean), indicating that increase (decrease) in specific humidity due to positive (negative) convergence of moisture transport decreases (increases) evaporation from the surface of the ocean; this is a reasonable explanation according to the bulk formula.

Likewise, the variation of the thermal advection and the subsequent convergence of the heat flux are highly correlated with the variation of downward longwave radiation and the lower tropospheric (850 hPa) temperature (see Fig. R2b). On the other hand, the small mean value of the convergence of the horizontal heat flux cannot explain the significant nonzero mean of the anomalous downward longwave radiation or the anomalous lower tropospheric (850 hPa) temperature. Thus, we think that the vertical process should be invoked to account for the significant changes in the means of the variables over the Barents-Kara Seas.

This is a serious issue and requires more detailed calculation and convincing demonstration, which we do not wish to pursue in the present study. We, however, acknowledge that we restrict ourselves to processes acting in the Arctic, ignoring the forcing from lower latitudes. [P3 L4-5: It should be noted that our discussion is restricted to processes in the Arctic; forcing from lower latitudes can also be important in the

C3

process of Arctic amplification and sea ice reduction.]

We showed the pattern of total cloud cover, since several authors address that radiative forcing produced by clouds is an important mechanism for Arctic amplification. As the reviewer mentioned, cloud liquid water and cloud ice water may be a better measure of the effect of clouds rather than total cloud cover. Figure R4 indeed shows the patterns of total cloud liquid water and total cloud ice water exhibit better consistency with the region of sea ice reduction. In lieu of this new finding, we will replace the pattern of total cloud cover by the patterns of TCLW and TCIW in Fig. 4. [P5 L17-21: The patterns of total cloud liquid water and total cloud ice water, which are the key variables for the formation of clouds, also exhibit a strong response over the region of sea ice reduction although their centers of action are shifted toward the Greenland Sea (Fig. 4d). The pattern of total cloud cover, however, does not show any strong cloud activity over the region of sea ice reduction (Fig. S3 in the supplementary information); it should be understood that cloud cover is a difficult variable to simulate accurately in a reanalysis model.]

C2: Atmospheric reanalyses include serious errors in the Polar regions. This is the case particularly for surface fluxes and near-surface meteorological variables (e.g. Jakobson et al., 2012; Tastula et al., 2013). Hence, to obtain more robust results, I suggest to repeat the calculations using a second reanalysis (e.g. NCEP-CFSR) in addition to ERA-Interim.

R2: In response to the reviewer's suggestion, we analyzed a limited number of variables from the NCEP reanalysis product in order to reproduce the key results in the present manuscript. Figure R5 shows the regressed loading vectors derived from the 1979-2016 NCEP reanalysis product with the sea ice loss mode as the target variable. As a comparison between Figs. R5 and R6 shows, there is no essential difference between the two sets of regressed loading vectors except for a small difference in the scales. This magnitude difference seems to be due to slightly different sensitivity of sea ice to atmospheric and oceanic forcing in the two datasets. This exercise confirms

C4

that the behavior of the atmospheric variables in association with the sea ice reduction in the Barents-Kara Seas is not significantly different between the two reanalysis products and the physical mechanism addressed in the present study is not overly sensitive to the choice of a model dataset.

Figure R7 further shows the daily variation of surface (2 m) air temperature, 850 hPa air temperature, upward longwave radiation and downward longwave radiation over the region of sea ice reduction (21° - 79.5° E \times 75° - 79.5° N). As a comparison between Fig. R7 and Fig. 6 in the manuscript shows, the daily variation of ERA-Interim derived from the NCEP reanalysis product is fairly similar to that derived from the ERA-Interim product. Again, there is a slight difference in the scales of anomalous variable, but the daily variation derived from the two datasets is not much different (see Figure 6 in the manuscript) confirming that the physical mechanism addressed in the present study is not sensitive to the choice of a dataset. We added the following statement. [P8 L8-11: Finally, it should be mentioned that the feedback process does not seem to be sensitive to a choice of the dataset. A similar experiment conducted by using the NCEP reanalysis data produces essentially identical results except for a slight overestimation of the strength of the anomalous patterns in Fig. 1a-f and Fig. 6 (see Figs. S5 and S6 in the supplementary information).]

C3: Several results detected from the reanalysis require a better physical explanation.

C3a: Lines 32-33: Why does the region of sea ice loss generate anticyclonic circulation? Figure 3 is not clear in this respect. Show maps of sea level pressure or geopotential height at a relevant pressure level to illustrate this and explain the physical mechanism resulting in an anticyclonic circulation.

R3a: Figures R8a and R8b show the winter-averaged patterns of SAT, and lower-tropospheric circulation associated with the sea ice loss mode. Figures R8c and R8d show the lower tropospheric vertical sections of temperature, geopotential height, and wind along 60° E and 80° N across the center of action. It is difficult to explain what ex-

C5

actly is happening dynamically based on data analysis alone. Nonetheless, the physical variables in Fig. R8 are physically consistent with each other. For example, the lower tropospheric wind field seems nearly in geostrophic balance with the geopotential height field. Further, Fig. R9 shows that the anomalous geopotential height field is nearly in hydrostatic balance with the anomalous temperature field:

$$(dZ)_j = -(RT_j)/g(d \ln p)_j,$$

where

$$(dZ)_j = Z_j - Z_{(j-1)}, T_j = ((T_j + T_{(j-1)}))/2, (d \ln p)_j = \ln p_j - \ln p_{(j-1)}.$$

Thus, it seems that the release of energy in the form of radiation and heat flux changes the temperature, and geopotential height in the lower troposphere adjusts in accordance with the hydrostatic balance. [new Figure 3: We replaced the 925 hPa air temperature pattern by the lower tropospheric geopotential height and wind pattern.] [P5 L6-8: Figure 3 shows the anomalous surface (2 m) air temperature, the lower tropospheric geopotential height and wind and the vertical section of anomalous temperature, geopotential height and wind along 60° E and 80° N associated with sea ice reduction.] [P5 L10-11: ... consistent according to the hydrostatic equation (see Fig. S2).] [We added relevant discussion in conjunction with Fig. R9 in the supplementary information together with the figure (see Figure S2 and corresponding explanation).]

C3b: Page 5, lines 29-30: if the turbulent surface fluxes are upward and net longwave radiation is upwards, they tend to reduce the Earth surface temperature but increase the near-surface air temperature, not decrease it.

R3b: We used the surface (2 m) air temperature as a proxy for the surface temperature, since there is no surface temperature variable in the ERA-Interim reanalysis product. Thus, we assumed that the atmosphere up to 2 m height from the surface essentially

C6

behaves the same way as the surface with a negligible absorption of turbulent heat flux. If the anomalous 2 m air temperature is not significantly different than surface temperature, the amount of anomalous net longwave radiation at 2 m level would not be much different from that at the surface. Therefore, there would be net deficit of radiation energy at the 2 m level, resulting in a decrease in surface air temperature. As the reviewer indicated, however, surface turbulent fluxes may be consumed to raise the 2 m air temperature although we do not know the amount of energy consumed at this level. Thus, we changed the sentence as follows: [P6 L8-9: This implies that surface air temperature should decrease, preventing further sea ice reduction.] See our discussion in Part (c) for more details.

C3c1: Page 6, lines 6-7: Why does a change in 2 m air temperature slightly lead the upward longwave radiation? Further, on lines 8-9: an increase in 2-m air temperature does not have a causal effect of increasing the upward longwave radiation (a statistical relationship may naturally exist). The upward longwave radiation at the surface (which is the product archived in ERA-Interim) is controlled by the surface temperature (and emissivity), not by the 2-m air temperature.

R3c1: It is difficult to answer why there is a lag between the two variables. In each grid box, upward longwave radiation is computed via (see Fig. R10)

$$ULR(t) = \epsilon_i(t)R(T_i(t))f_i(t) + \epsilon_o(t)R(T_o(t))f_o(t), \quad (1)$$

where $R(t)$ is radiation as a function of radiating temperature T , ϵ is emissivity, f is a fractional area, the subscripts i and o stand for the “ice-covered” and “open (ice free)” areas, respectively, and $ULR(t)$ denotes the averaged upward longwave radiation in the grid box. In (1), the radiating function (basically Planck function) is a nonlinear function of temperature, and the emissivity ϵ may be dependent upon the sky condition as well as the surface condition. Further, f varies in time. Thus, the calculation of upward longwave radiation in each grid box may not be a linear function of (grid-averaged)

C7

surface temperature. This means that anomalous upward longwave radiation is not a linear function of anomalous surface temperature. Also note that the amount of anomalous radiation is not a function of anomalous temperature; it is determined by the temporally varying background (mean) temperature plus the anomalous temperature. Therefore, the amount of anomalous upward longwave radiation is not simply a function of anomalous surface temperature.

The 2 m air temperature change slightly leads the change in upward longwave radiation according to our lagged correlation analysis based on the 3-hourly ERA-Interim data. As can be seen in our original Figure 7 in the manuscript, however, the lead is less than 0.1 days (less than one time step) and the lagged correlation varies little between the lag range of [0, 0.1] day. Thus, we cannot confirm if this lead/lag relationship is a realistic relationship between the two variables or an artifact of analysis. Based on the shape of the lagged correlation (correlation for positive lags is generally stronger than that for negative lags at the same distance from lag 0), we thought that it was reasonable to say that 2m air temperature slightly leads upward longwave radiation.

We used the 2 m air temperature as a proxy for the surface temperature in order to explain changes in upward longwave radiation. As the reviewer mentioned, surface temperature instead of surface air temperature should be used in order to address this issue. Unfortunately, there is no variable called the “surface temperature” in the ERA-Interim product. We could have used the skin temperature T_{SK} but it is defined as the temperature of the surface at radiative equilibrium:

$$R_{SW} + R_{LW} + J_s + L J_q = \Lambda_{skin}(T_{SK} - T_S), \quad (2)$$

where R_{SW} and R_{LW} are shortwave and longwave radiation fluxes at the surface, J_s and J_q are heat and moisture fluxes, Λ_{skin} is skin conductivity, T_S is temperature of soil, snow or ice. It is a poor reflection of radiative energy surplus or deficit at the surface, since any surplus/deficit of radiative energy is compensated by turbulent fluxes and/or

C8

heat conduction between the level of skin temperature and the underlying soil, snow or ice. Further, skin temperature is identical with sea surface temperature over ice-free regions. Thus, change in net longwave radiation is not reflected in the skin temperature over the open ocean.

The use of skin temperature does not improve the interpretation of the analysis results. As seen in Table R1, skin temperature is slightly better correlated with upward longwave radiation, but exhibits much poorer correlation with downward longwave radiation, net longwave radiation or 850 hPa air temperature for the sea ice loss mode. As seen in Fig. R11, the spatial patterns of the two variables are essentially identical particularly over the region of sea ice reduction in the Barents-Kara Seas. Thus, the use of skin temperature instead of surface air temperature does not alter or improve the physical interpretation of the analysis results in the present study. Neither could we confirm that surface air temperature leads the upward longwave radiation, nor could we find a suitable variable to replace the surface temperature. Therefore, only option we have is to remove the statement about the lead/lag relationship between the surface air temperature and the upward longwave radiation. We modified Figs. 7b and 8, and the corresponding discussion as follows. [P6 L21-22: ... downward longwave radiation, which leads to a sea ice reduction. As a result, surface temperature and upward longwave radiation may increase.] [new Figure 7b Figure 8]

Table R1. Correlation of the loading vectors of 850 hPa air temperature (T850), upward longwave radiation (ULW), downward longwave radiation (DLW), and net longwave radiation (NLW) with surface air temperature (SAT) in the second column and with skin temperature (SKT) in the third column.

	T850	ULW	DLW	NLW
SAT	0.861	0.878	0.916	0.681
SKT	0.448	0.891	0.722	0.286

C9

C3c2: Further, on line 10: Instead of a causal effect from upward longwave radiation to sea ice concentration change, a reduction of sea ice concentration in winter must have an immediate effect in strongly increasing the upward longwave radiation.

R3c2: We agree with the reviewer. We used the increased upward longwave radiation as an evidence of the increased surface temperature, which eventually leads to sea ice reduction. As the reviewer mentioned, however, sea ice reduction immediately increases the upward longwave radiation because of the exposure of higher sea surface temperature. Thus, the lead/lag relationship between the upward longwave radiation and sea ice reduction is not so straightforward. We removed the following sentence: [P6 L22: Further, both downward and upward longwave radiation changes seem to lead sea ice concentration change.] At the same time, we modified Figure 8 to reflect this change. [new Figure 8]

C3d: Page 6, line 13: related to the above, I suggest removing the words "surface air temperature increases and".

R3d: We followed the suggestion of the reviewer. [P6 L25: As a result, surface air temperature increases and sea ice melts]

Minor comments

C1: Page 2, line 7: I think Vihma (2014) should be dropped from this line.

R1: We removed the Vihma (2014) reference. [P2 L7: Vihma (2014) is removed now.]

C2: Page 2, lines 13-17: During spring and early summer the albedo decreases from roughly 0.85 of dry snow-covered ice to 0.4 of melting ice. Hence, the albedo feedback is important already during the snow and ice melt, already before the appearance of open sea.

R2: We modified the sentence as follows: [P2 L17-18: ... absorbing atmospheric heat during summer. The albedo feedback is also important during the snow and ice melt in spring and early summer even before the appearance of open sea.]

C10

C3: Page 2, line 18: the term “oceanic heat transport” is not the best possible, as it may be interpreted as the horizontal transport from lower latitudes to the Arctic.

R3: We modified the sentence as follows: [P2 L19-20: ... mechanism becomes oceanic horizontal advection and vertical convection of heat (Screen and Simmonds, 2010b).]

C4: Equation 1 and the text below: explain what is r .

R4: We modified the sentence as follow: [P3 L16: ... physical process, describes ... on a longer time scale, and r and t denote location and time, respectively.]

C5: Page 4, line 23: On the basis of Figure 2, I would not write that the sea ice concentration remains nearly stationary throughout the winter.

R5: We modified the sentence as follows: [P5 L1-2: Sea ice concentration varies slightly on a daily basis, and its fluctuation is less than 2% from the mean value of -14.7% throughout the winter (Fig. 2).]

C6: Page 4, line 25: I cannot detect the 40% decrease from the amplitude time series. Also, better explain what the amplitude represents.

R6: As shown in (1), actual data is obtained by multiplying each loading vector with corresponding PC (amplitude) time series. According to Fig. 1g, the amplitude time series has increased by about 2.6 during the 37-year period. Multiplying this value with 14.7% (loading vector; Fig. 2), we obtain $\sim 38.2\%$. Actually, Fig. 1h is obtained by multiplying the PC time series Fig. 1g with the corresponding loading vector Fig. 2. We modified the sentence as follows: [P5 L3-5: Multiplying the amplitude (PC) time series (Fig. 1g) with the loading vector (Fig. 2) of the sea ice loss mode as in (1), actual sea ice concentration time series is obtained as in Fig. 1h. According to Fig. 1h, sea ice concentration has decreased by $\sim 40\%$ during the last 37 years.] [Figure 1 caption: ... The red curve in Fig. 1h is obtained by multiplying the loading vector of sea ice concentration (Fig. 1a) averaged in the boxed area with the amplitude time series (Fig.

C11

1g) according to (1). ...]

C7: Page 5, line 9: “the little connectivity” between sea ice reduction and total cloud cover may originate from the fact that sea ice reduction generates two effects that compete against each other: increased latent heat flux tends to increase cloudiness but increasing sensible heat flux tends to reduce it.

R7: We thank the reviewer for enlightening us. As mentioned in our response to your major comments, we included the total cloud pattern since several authors mention the possible role of clouds for Arctic amplification. See our response to Major Comment 1 above.

C8: Page 6, lines 23-25: These are interesting numbers. Please, confirm if these are winter means in 1979-2016 averaged over sea areas north of 60N. It might be interesting to compare them against results of Lupkes et al. (2008), which show air temperature responses to 1% reduction in sea ice cover in different conditions.

R8: It is the result based on the average over the region of sea ice reduction (21° - 79.5° E \times 75° - 79.5° N) in the Barents-Kara Seas; it shows the values of anomalous radiation and surface fluxes for an average sea ice reduction of $\sim 15\%$ (see Fig. 2). Lüpkes et al. (2008) conducted experiments in different settings using a 1D atmospheric model coupled with snow/sea ice model. Therefore, a rigorous comparison is impossible. Our numbers are smaller than those in Lüpkes et al. but are of the same order of magnitude. It is difficult to explain the reasons for this difference, but the absence of horizontal advection is a plausible cause. In the presence of horizontal advection, anomalous temperature and fluxes over sea ice leads are quickly diffused, resulting in reduced local maxima. We can see a hint of horizontal advection in Fig. 1 in the manuscript; while turbulent heat flux is nearly confined to the area of sea ice loss, 2 m air temperature and other variables are smoothed out over a much wider area. We would rather not include this discussion in the revised text, since we eliminated 2 m air temperature increase in the feedback loop. Moreover, our explanation above is

C12

somewhat premature and conjectural in nature. [no modification]

C9: Figure 2. Is plot (a) needed at all, as the same line appears in plot (b)?

R9: We removed Figure 2a. [new Figure 2]

C10: Figure 4. Add information on colour scales and absolute values. Only the contour intervals are given.

R10: We revised Figure 4 in order to provide the necessary information the reviewer asked. [new Figure 4; figure caption: The red contour is drawn at the value of the contour interval.]

C11: Figure 5. Does the shading represent sea ice concentration in all four plots? If yes, why it includes small differences between the plots?

R11: We accidentally used different shading interval for the sea ice concentration field in Fig. 5c. We corrected the figure. [new Figure 5]

C12: Figure 6. Explain better how the time series in days should be interpreted. It cannot be the mean over 1979-2016. Is it from some selected year?

R12: It is the plot of regressed loading vector $B_1(r, t)$ of the sea ice loss mode averaged over the region of sea ice loss ($21^\circ\text{-}79.5^\circ\text{E} \times 75^\circ\text{-}79.5^\circ\text{N}$) for different variables. The daily time series are interpreted as typical winter variation of surface fluxes and radiation associated with the sea ice reduction in Fig. 2. Actual data associated with the sea ice loss mode is obtained by multiplying the loading vector with the corresponding PC time series, i.e., the space-time evolution pattern associated with the sea ice loss mode is $T^{(1)}(r, t) = B_1(r, t)T_1(t)$. Thus, the typical time series of surface fluxes and radiation depicted in Fig. 6 are amplifying according to Fig. 1g. We added more description on this figure. [P5 L28-30: Figure 6 shows the winter daily variations of the regressed loading vectors in (6) (terms in curly braces) averaged over the region of sea ice reduction ($21^\circ\text{-}79.5^\circ\text{E} \times 75^\circ\text{-}79.5^\circ\text{N}$); it may be interpreted as the atmospheric response to the sea ice reduction shown in Fig. 2.]

C13

C13: Figure 8. Referring to my previous comments, I suggest dropping “2m T increase (0.24)” from the figure, and drawing an arrow directly from increased LW-down to sea ice reduction. Otherwise, provide a good explanation on the causality of the link.

R13: We followed the suggestion of the reviewer. [new Figure 8]

** The combined response file including a marked-up manuscript is attached.

References: Jakobson, E., T. Vihma, T. Palo, L. Jakobson, H. Keernik, and J. Jaagus (2012). Validation of atmospheric reanalyses over the central Arctic Ocean, *Geophys. Res. Lett.* 39, L10802, doi:10.1029/2012GL051591. Tastula, E.-M., T. Vihma, E. L. Andreas, and B. Galperin (2013), Validation of the diurnal cycles in atmospheric reanalyses over Antarctic sea ice, *J. Geophys. Res. Atmos.*, 118, 4194–4204, doi:10.1002/jgrd.50336.

Please also note the supplement to this comment:

<https://www.the-cryosphere-discuss.net/tc-2017-39/tc-2017-39-AC1-supplement.pdf>

Interactive comment on The Cryosphere Discuss., <https://doi.org/10.5194/tc-2017-39>, 2017.

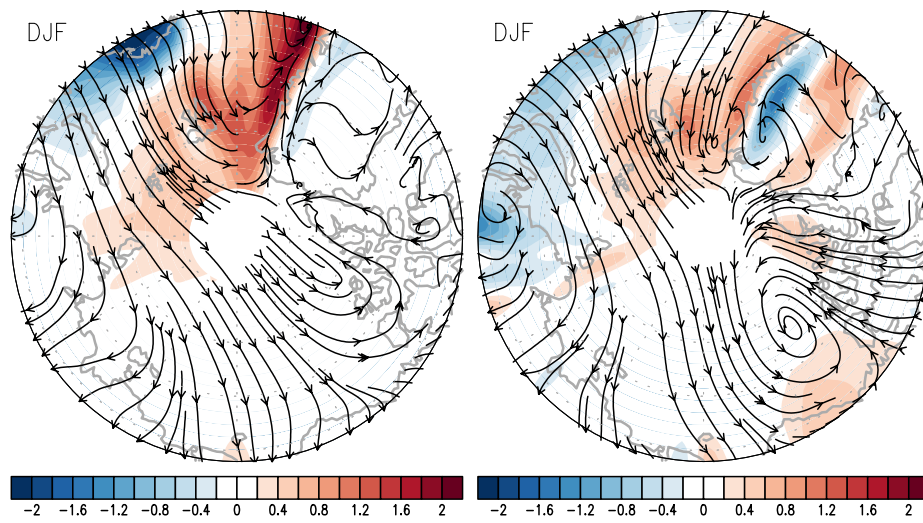


Fig. 1. Winter-averaged (left panel) moisture transport (streamline) and its convergence (shade) and (right panel) heat transport (streamline) and its convergence (shade) in the lower troposphere

C15

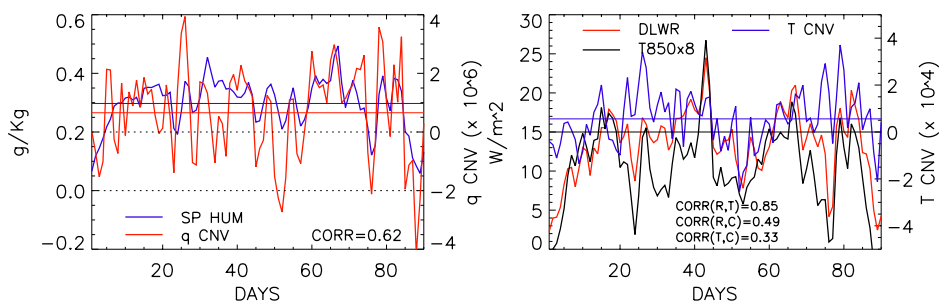


Fig. 2. The daily time series of anomalous specific humidity and anomalous moisture convergence averaged over the sea ice loss region (21° - 79.5° E \times 75° - 79.5° N) in the Barents-Kara Seas. These ti

C16

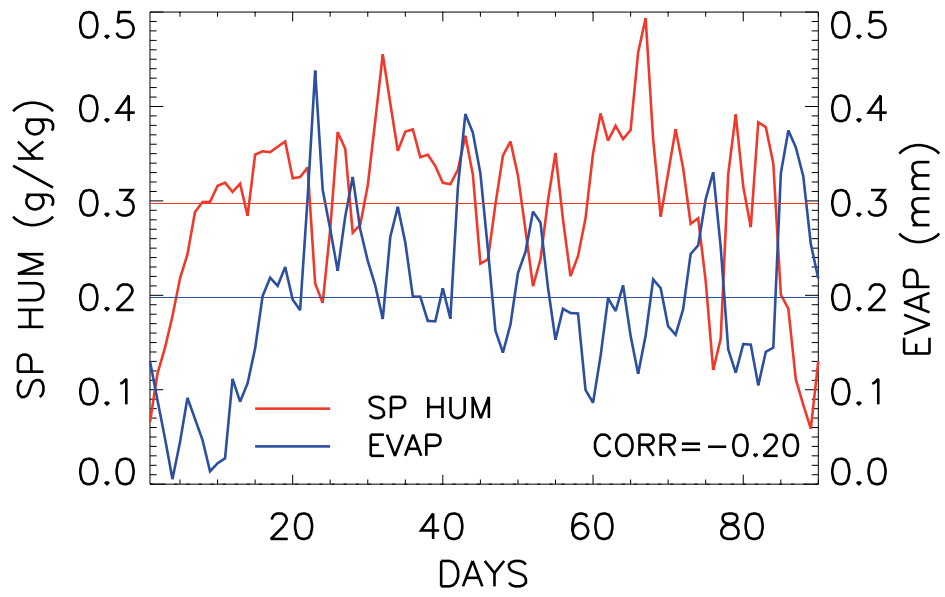


Fig. 3. The daily variation of specific humidity (red) and evaporation (blue) averaged over the region of sea ice reduction (21° - 79.5° E \times 75° - 79.5° N) in the Barents-Kara Seas.

C17

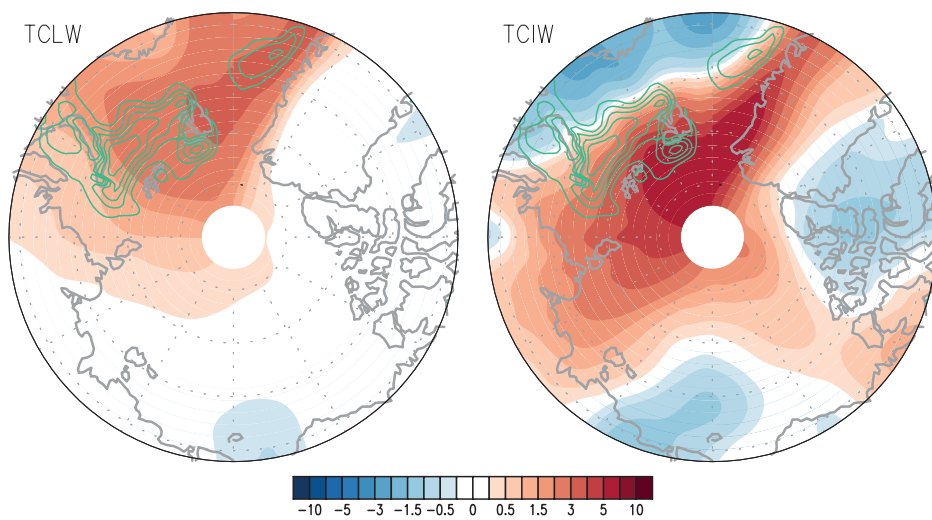


Fig. 4. The winter-averaged patterns of total cloud liquid water (left) and total cloud ice water (right) associated with the sea ice loss mode.

C18

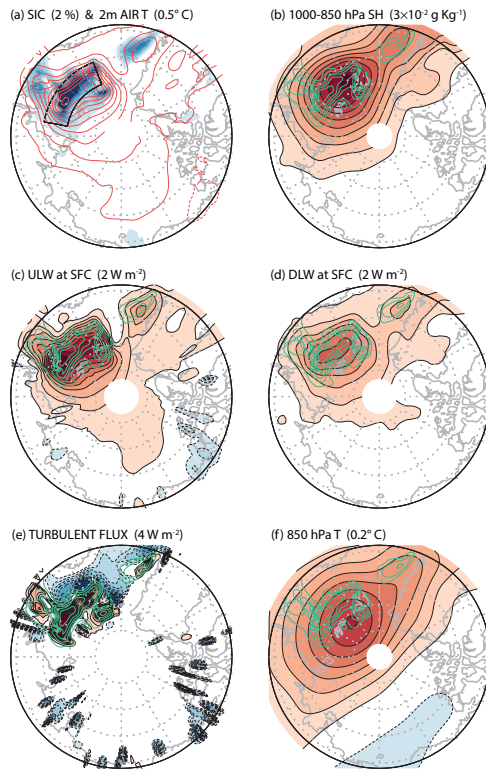


Fig. 5. The regressed patterns of atmospheric variables based on the NCEP Reanalysis product (1979-2016). The target is the sea ice loss mode.

C19

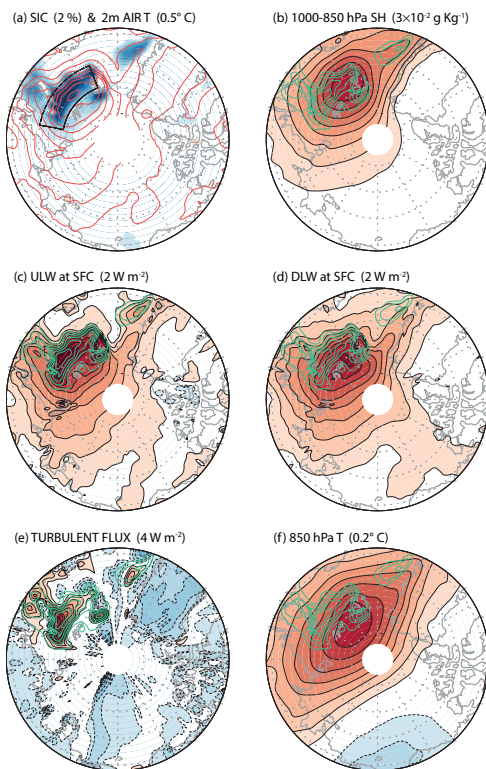


Fig. 6. The regressed patterns of atmospheric variables based on the ERA-Interim reanalysis product (Figure 1a-f in the manuscript).

C20

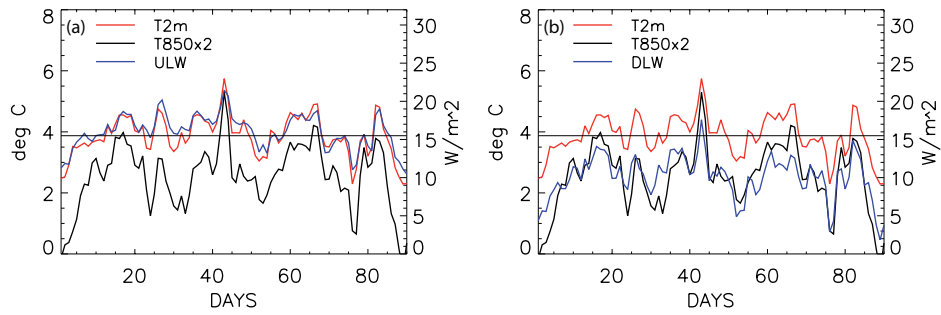


Fig. 7. Daily pattern of variability over the region of sea ice loss (21° - 79.5° E \times 75° - 79.5° N) derived from the NCEP reanalysis data: (a) 2 m air temperature (red), 850 hPa air temperature \times 2 (black), and u

C21

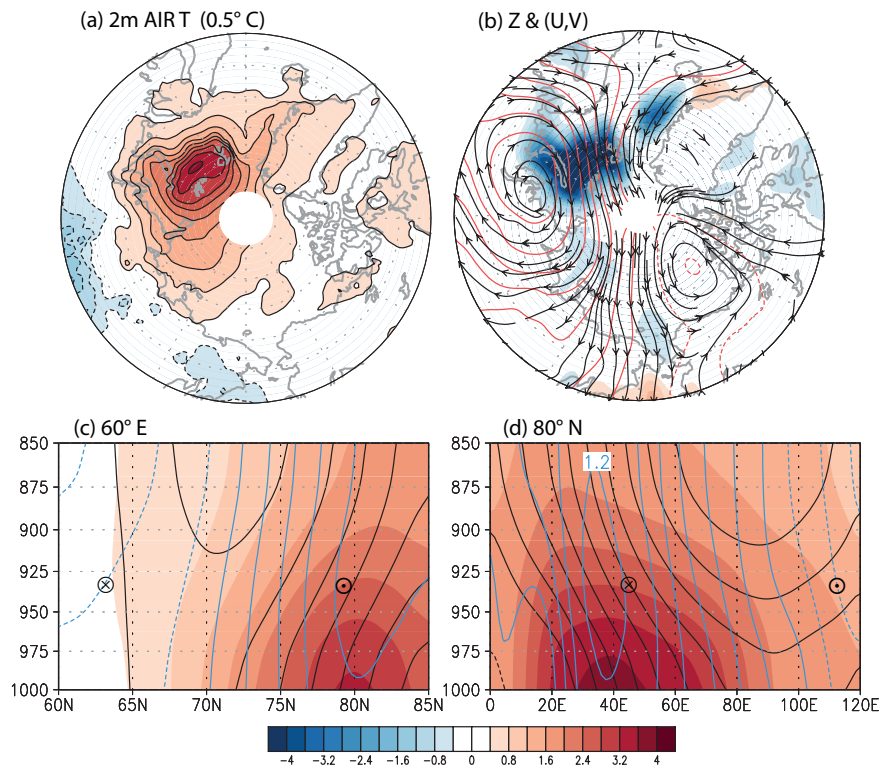


Fig. 8. The spatial patterns (60° - 90° N) of (a) 2 m air temperature, and (b) lower tropospheric (1000-900 hPa) geopotential height (red contour) and wind (streamline). (c and d) The lower tropospheric vertic

C22

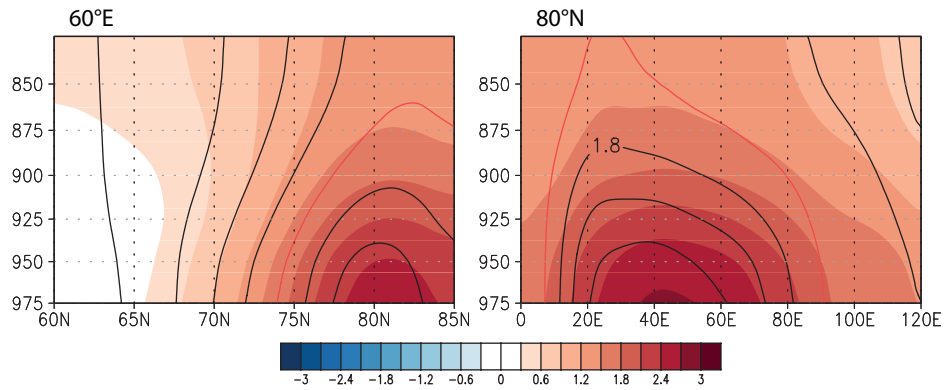


Fig. 9. The pressure layer thickness ($\Delta Z=Z(p_1)-Z(p_0)$) derived from the geopotential height pattern in Fig. R8 (shade) and that derived from the hydrostatic equation (contour). The red contour represents

C23

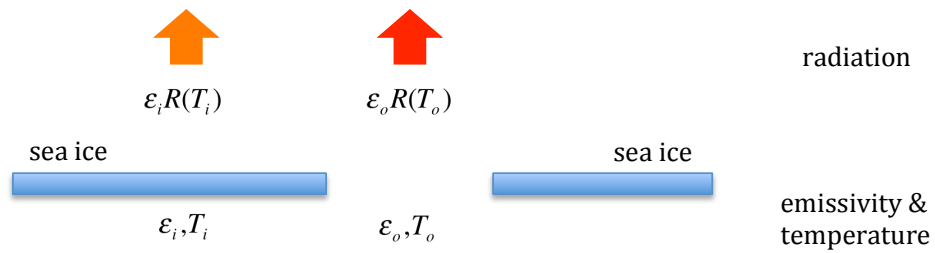


Fig. 10. A typical situation of calculating upward longwave radiation in each grid box. Upward longwave radiation is calculated for sea ice tile and open ocean tile separately in order to calculate total upwa

C24

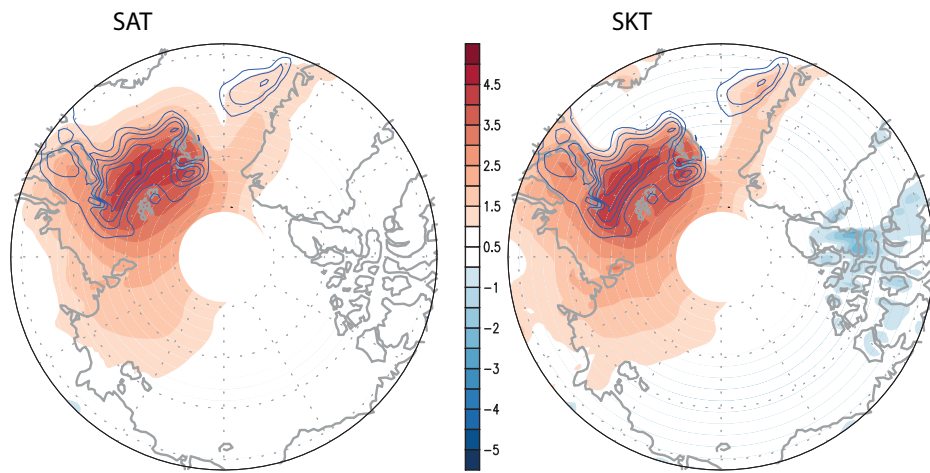


Fig. 11. The regressed patterns of surface air temperature (SAT) and skin temperature (SKT) with the sea ice loss mode as the target (contour).